International Journal on Recent and Innovation Trends in Computing and Communication
ISSN: 2321-8169 Volume: 11 Issue: 7s
DOI: https://doi.org/10.17762/ijritcc.v11i7s.7026
***Article Received**: 04 April 2023 **Revised:** 25 May 2023 **Accepted:** 05 June 2023*

Multi-Scale Hybrid Spectral Network for Feature Learning and Hyperspectral Image Classification

Easala Ravi Kondal[1], Soubhagya Sankar Barpanda[2]
[1]School of Computer Science and Engineering
VIT-AP University
Amaravati, India.
easala.ravikondal@gmail.com
[2]School of Computer Science and Engineering
VIT-AP University
Amaravati, India.
soubhagya.barpanda@vitap.ac.in

Abstract— Hyperspectral image (HSI) classification is an important concern in remote sensing, but it is complex since few numbers of labelled training samples and the high-dimensional space with many spectral bands. Hence, it is essential to develop a more efficient neural network architecture to improve performance in the HSI classification task. Deep learning models are contemporary techniques for pixel-based hyperspectral image (HSI) classification. Deep feature extraction from both spatial and spectral channels has led to high classification accuracy. Meanwhile, the effectiveness of these spatial-spectral methods relies on the spatial dimension of every patch, and there is no feasible method to determine the best spatial dimension to take into consideration. It makes better sense to retrieve spatial properties through examination at different neighborhood scales in spatial dimensions. In this context, this paper presents a multi-scale hybrid spectral convolutional neural network (MS-HybSN) model that uses three distinct multi-scale spectral-spatial patches to pull out properties in spectral and spatial domains. The presented deep learning framework uses three patches of different sizes in spatial dimension to find these possible features. The process of Hybrid convolution operation (3D-2D) is done on each selected patch and is repeated throughout the image. To assess the effectiveness of the presented model, three benchmark datasets that are openly accessible (Pavia University, Indian Pines, and Salinas) and new Indian datasets (Ahmedabad-1 and Ahmedabad-2) are being used in experimental studies. Empirically, it has been demonstrated that the presented model succeeds over the remaining state-of-the-art approaches in terms of classification performance.

Keywords- Deep learning; Multiscale; 3D-2D Convolutional; Classification; Hyperspectral image; Spectral-spatial information.

I. INTRODUCTION

The trustworthiness of results from hyperspectral image (HSI) analysis has made it a popular topic of study for a plenty of earth monitoring applications, including military, environmental, mining, medical fields, and many others [1-3]. Hyperspectral image classification is a challenging task due to the minimal amount of labelled training examples and the high dimensional space that includes a wide range of spectral bands. Conventional image classification methods, such as SVM and KNN classifiers, have performed well for this challenge because they can compensate for the extensive spectrum information acquired in hyperspectral images [4].

This research has been extensively reviewed in the studies [5-7]. Convolutional neural network (CNN)-based algorithms had recently obtained exceptional achievement for different image analysis-associated works, such as object identification and image classification, since enormous accomplishment of deep learning. In the literature [8], various supervised classifiers for HSI classification have developed. The extraction of features using deep convolutional neural network (CNN) methods had been shown to enhance the classification accuracy of HSI. The key element to achieving a high degree of classification precision is the acquisition of distinctive spatial-spectral features [9-11]. The spectral-spatial viewpoints must be chosen into consideration while classifying hyperspectral images.

A hyperspectral image, also known as a spectral perspective image, is conceptually made up of numerous of smaller "images," every of which signifies a certain wavelength band of the electromagnetic spectrum. Consequently, 3D spectral-spatial data are typically used to represent hyperspectral images. While hyperspectral images capture objects from various perspectives, current CNN-based techniques [12] [13] that only consider spatial or spectral information necessarily ignore the entwined relationships between the pair. In essence, the interconnecting information can be utilized to enhance categorization achievement. Consequently, it is possible to train a comparatively good CNN-based classifier using only a small amount of labelled 3D spectral-spatial images. Meanwhile, the effectiveness of these spatial-spectral methods relies on the spatial size of every patch, and there is no feasible method to determine the best spatial size to take into consideration. It

International Journal on Recent and Innovation Trends in Computing and Communication
ISSN: 2321-8169 Volume: 11 Issue: 7s
DOI: https://doi.org/10.17762/ijritcc.v11i7s.7026
***Article Received**: 04 April 2023 **Revised:** 25 May 2023 **Accepted:** 05 June 2023*

makes better sense to retrieve spatial properties through examination at different neighborhood scales in spatial dimensions.

There have been several early attempts in this direction to model spectral-spatial information simultaneously [14] [15]. These methods, referred to as 3D-CNN models, employ arrayed convolution activities on spectral-spatial feature region in a layer-by-layer fashion. The benefit of this particular 3D-CNN approach is seen in the produced feature maps. The fundamental drawback of these methods is that because the public HSI datasets are so limited, it is impractical to build a deep 3D-CNN method since more training instances are needed.

We proposed a multi-scale hybrid spectral CNN (MS-HybSN) model for HSI classification. In the presented MS-HybSN, distinct spatial contexts of a particular pixel are examined to produce multi-scale 3D patches for the network to obtain spectral- spatial properties from the HSI. As can be observed in Figure. 1, the MS-HybSN model incorporates three Hybrid CNNs parallelly to retrieve deep spectral-spatial features from each network and all retrieved features are fused to fed to the fully-connected layers for further classification. As shown in Fig. 2, in the presented model, every HybSN is a combination of spatial-spectral 3DCNN and spatial 2DCNN. The 3DCNN optimizes the representation of combined spectral-spatial properties from a bundle of spectral channels. The 2DCNN built on above of the 3DCNN gains higher-level abstraction spatial modelling. As well, compared to using a 3DCNN alone, the usage of hybrid CNNs lowers the model's difficulty. It has been shown through experimental outcomes on benchmark dataset that the introduced MS-HybSN succeeds over various state-of-the-art HSI classifiers. The subsequent summarizes the contributions of the work:

- Distinct spatial contexts of a particular pixel are examined to produce multi-scale 3D patches to acquire the significant features from HSI to enhance classification accuracy.
- Significant experiments were performed on publicly available datasets, and encouraging outcomes illustrate that the presented MS-HybSN outperforms other contemporary HSI classifiers.

Here is how the remainder of the paper is laid out: The review of the literature for the proposed work is mentioned in Section II, and the model architecture is presented in Section III. The experimental research, outcomes and conversations of the proposed framework are stated in Section IV. Finally, Section V presents the inferences.

II. RELATED WORK

It is widely acknowledged in the research community that classifying hyperspectral images is a significant problem in the field. However, earlier research mostly focused on traditional computational techniques. We quickly cover the most recent deep learning pixel-based models in this section.

A 2D-CNN pixel--based method was presented in [13] to retrieve the spectral-spatial data embedded in HSIs, where 2D-CNN has been used to examine the band selection outcomes. A variety of pixel--based techniques were put forth to combine specific 2D-CNN models for the classification of HSI based on the band selection outcomes. As an illustration, Liu et al. [16] used deep belief networks to retrieve deep spectral characteristics. A 2D-CNN adaptive HSI classification model has been presented by Zhu [17] and is composed of adaptable convolutions and down sampling which integrate the underlying information of every input sequence in an adaptive manner. Through the addition of three feature regions based on spectrum information to spatial regions, in [18], Han developed a 2D-CNN method to assess spectral-spatial characteristics. Zhao and Du [19] gave an example of a spectral-spatial feature-based categorization method that utilises a 2DCNN to collect spatial data and a linear local distinction encase to find spectral data. Although these methods might produce models with comparable performance, they required a huge training dataset, which is not feasible for the majority of real-world implementations.

There are techniques that account the spatial-spectral features of the HSI data. As CNN models are so flexible, a wide range of methods and networks can be created to do spectral-spatial analysis. Chen [20] presented a deep 3D-CNN model comprised of multiple 3D convolutional layers that extracted spectral–spatial characteristics for classification. Similar to this, Lee [21] proposed a deep network with such an emphasis on 3D data. The proposed model is capable of accurately capturing alterations in local impulses stated in spectral-spatial data. In order to evaluate a series of volumetric models of the HSI, Hamida [22] devised and assessed a set of 3D schemes that combine the conventional 3D convolution operations to enable a joint spatial-spectral information analysis. Kanthi [23] presented a 3D-CNN method that splits HSI into 3D regions and pulls deep spectral-spatial data for HSI classification.

However, certain hybrid approaches incorporated 2D-CNNs and 3D-CNNs. For example, Roy [24] proposed HybridSN model that merges spectral and spatial 3D-CNN with spatial 2D-CNN. Raviteja [25] established hierarchical image fusion model for HSI classification to merge specified spectral features into image groups. Wan [26] presented multiscale graph convolutional network for irregular image region convolution for HSI classification. Meng [27] employed connections with feed-forward shortcuts to access all convolutional layers' hierarchical input to create a dense multiscale hybrid network

International Journal on Recent and Innovation Trends in Computing and Communication
ISSN: 2321-8169 Volume: 11 Issue: 7s
DOI: https://doi.org/10.17762/ijritcc.v11i7s.7026
***Article Received**: 04 April 2023 **Revised:** 25 May 2023 **Accepted:** 05 June 2023*

and a multi-scale HSI spatial and spectral HybridCNN was presented by Mohan [28] for Classification tasks. Kanthi [29] introduced a deep CNN model that uses three distinct multi-scale spatial-spectral regions to retrieve features from both the spatial and spectral bands.

In contrast to 2D-CNN and 3D-CNN based models, multiscale hybrid pixel-based models certainly contain more features. As a result, the 3D-CNN based models have substantially higher network complexity and memory requirements than the 2D-CNN based methods. This seeming inability to directly apply these 3D-CNN based approaches to model such entangled interactions can be attributed to the following. It is challenging to optimize the prediction loss via these nonlinear design since majority of present 3D-CNN based techniques contain multiple 3D convolutional layers. Deep feature extraction from both spatial and spectral channels has led to high classification accuracy. Meanwhile, the effectiveness of these spatial-spectral methods relies on the spatial size of every patch, and there is no feasible method to determine the best spatial size to take into consideration. It makes better sense to retrieve spatial properties through examination at different neighborhood scales in spatial sizes. In this context, we motivated in this direction to present a MS-HybSN model that uses three distinct multi-scale spatial-spectral patches to pull out features in spectral and spatial domains.

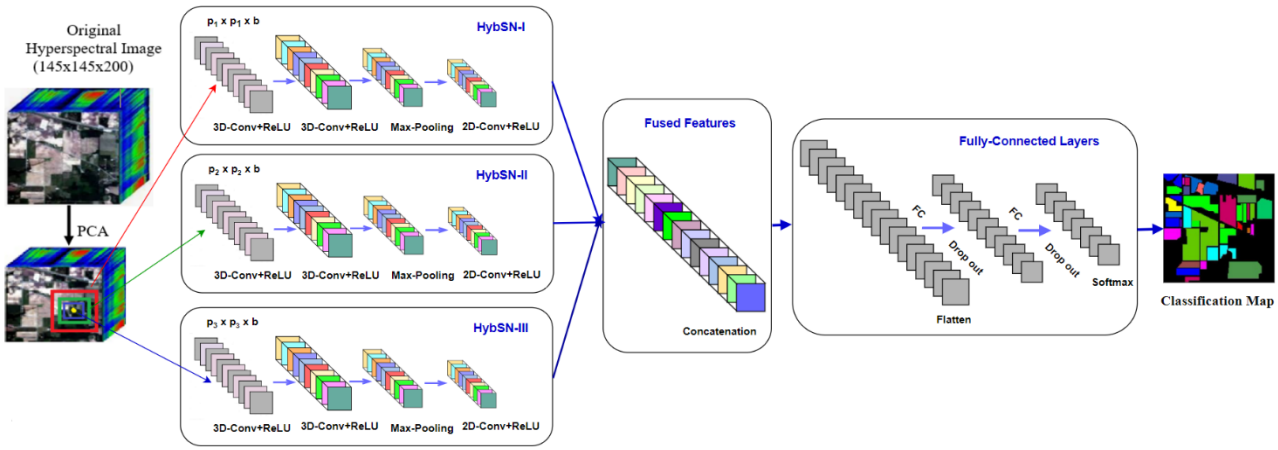

Figure. 1 Overview of the presented multiscale HybSN (MS-HybSN) network.

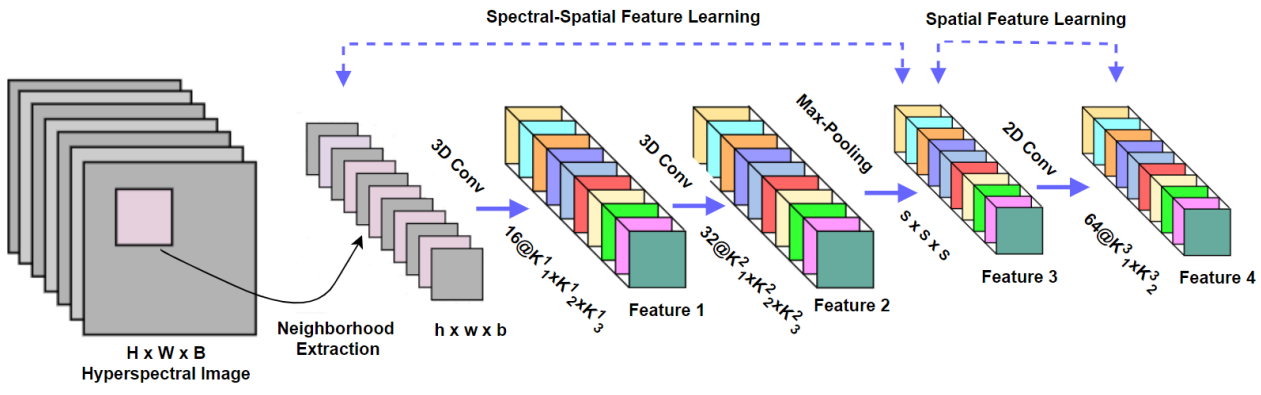

Figure. 2 Integration of 3D-2D convolution for feature learning.

III. Proposed Methodology

In this section, we provide in detail the presented multiscale hybrid spectral network (MS-HybSN) method. As seen in Figure 1, the presented approach MS-HybSN employs multiscale 3-D patches as input to generate integrated spectral-spatial features from the provided HSI. Assume that the provided HSI may be seen as a 3D cube with the dimensions W x H x B, in which W, H indicate the spatial height and width of the image, and B represents the number of spectral channels.

As with the most popular CNN architectures that already exist [18, 23, 25, 29, 30], the no. of channels was decreased initially using PCA, and 30 spectral bands were chosen for the IP and 15 spectral channels were chosen for other datasets employed in exploratory investigation.

International Journal on Recent and Innovation Trends in Computing and Communication
ISSN: 2321-8169 Volume: 11 Issue: 7s
DOI: https://doi.org/10.17762/ijritcc.v11i7s.7026
***Article Received**: 04 April 2023 **Revised:** 25 May 2023 **Accepted:** 05 June 2023*

The presented framework MS-HybSN retrieves spatial-spectral features for particular pixels in the pattern of multiscale 3D-patches in three distinct spatial contexts. As depicted in Fig. 1, these multiscale 3D-patches are supplied to three HybSN networks. Each patch has the dimensions p_ix p_ix d, where p_i is the height and width of patch i, d is the patch depth and i is number of patches associated with a single pixel. The RAM of 25.51 GB Google Colab Pro GPU is used for all experiments in the current work. According to this setup, selected optimised three patches with sizes p_1 x p_1 x $d = 15$ x 15 x 30 , p_2x p_2x $d = 13$ x 13 x 30 , and p_3x p_3x $d = 11$ x 11 x 3 . As presented in Figure 2, every HybSN is a combination of spectral-spatial 3DCNN and spatial 2DCNN. The 3DCNN optimizes the representation of combined spatial-spectral features from a bundle of spectral channels.

The 2DCNN built on above of the 3DCNN gains higher-level abstraction spatial modelling. Every HybSN network contains two 3D convolution layers ($3D - Conv_1$ and $3D - Conv_2$), max pooling layer ($3D - Pool$) and two sets of filters $K_1 = 16$ and $K_2 = 32$ having size 3 x 3 x 7 *and* 3 x 3 x 5 respectively in 3D-Convolution process and one 2D convolution layer ($2D - \text{Conv}$) with filter $K_3 = 64$ having size 3 x 3 in 2D-Convolution process. Batch normalisation layer and activation function ReLU is used after each convolutional layer. The max-pool layer with stride 2 x 2 x 2 a is aplied after the second 3D convolutional layer as Equation. (1).

$$f(x) = \begin{cases} 0, & x < 0 \\ x, & x \geq 0 \end{cases} \qquad (1)$$

The extracted features from multiple spatial context levels are reshaped and flattened before being given to the fully connected layers fcl_1, fcl_2, and fcl_3 for classification. As a regularization strategy, the dropout layer was applied at a rate of 0.5% after each fully-connected-layer to remove the overfitting issue when training samples were few.

Each neuron's activation function in a fully connected layer is calculated using Equation (2).

$$Act_x(fcl) = g(w_x(fcl) * act_{x-1}(fcl) + b_x) \qquad (2)$$

Where, $w_x(fcl)$ is the weighted total of all the inputs to the precedent layer and b_x is the bias. $g(.)$ is a representation of the ReLU activation.

Finally, the data is classified using a soft-max probabilistic model. $F = [F_x]$x, where x is a positive integer between 1 and n, represents the feature representations after the entire model has been implemented, as in Equation (3).

$$\text{Smax}\,(F)_x = \frac{e^{Fx}}{\sum_{x=1}^{k} e^{Fy}} \text{ for } x = 1,2,3,..,n \qquad (3)$$

At last, there is the argmax function (maximum arguments). It establishes the location in the region of a function where the functional parameters are at their highest. Equation (3) can be used to allocate classes to a m number of hyperspectral image class labels ranging from $Q = \{1, 2, 3, 4, .\ .\ , m\}$.

TABLE I. DESCRIPTION-BENCHMARK AND INDIAN HSI DATASETS.

Parameters	**SA**	**PU**	**IP**	**AH-1**	**AH-2**
Sensor	AVIRIS	ROSIS	AVIRIS	AVIRIS-NG	AVIRIS-NG
Wavelength Range	360–2500 µm	0.43–0.86 µm	0.4–2.5µm	0.37–2.5µm	0.37–2.48 µm
No. of Classes	16	9	16	5	7
No. of Spectral Bands	200	115	200	351	370
Spatial Dimension	512 × 217	610 × 340	145 ×145	300 × 200	300 × 200

TABLE II. PROPOSED MODEL CLASSIFICATION ACCURACIES (IN %) ON BENCHMARK DATASETS.

Model	**SA**			**PU**			**IP**		
	AA	**OA**	**Kappa**	**AA**	**OA**	**Kappa**	**AA**	**OA**	**Kappa**
2D-CNN [7]	94.63	94.94	94.23	92.86	93.18	92.03	88.29	91.69	90.65
3D-CNN [7]	97.07	96.98	96.38	96.12	96.54	95.53	94.59	95.14	93.99
HybridSN [25]	99.59	99.85	99.52	99.03	99.93	99.81	98.56	99.22	99.12
HybridCNN [29]	99.87	99.95	99.98	99.98	99.99	99.99	99.72	99.80	99.76
MS-3DCNN [30]	99.98	99.99	99.98	99.97	99.99	99.99	98.87	99.89	99.24
Proposed Method	99.99	99.99	99.98	99.98	99.99	99.99	99.13	99.98	99.92

International Journal on Recent and Innovation Trends in Computing and Communication
ISSN: 2321-8169 Volume: 11 Issue: 7s
DOI: https://doi.org/10.17762/ijritcc.v11i7s.7026
***Article Received**: 04 April 2023 **Revised:** 25 May 2023 **Accepted:** 05 June 2023*

TIBLE III. PROPOSED MODEL CLASSIFICATION ACCURACIES (IN %) ON INDIAN DATASETS.

Model	AH-1			AH-2		
	AA	OA	Kappa	AA	OA	Kappa
3D-CNN [7]	82.41	80.99	78.17	69.30	70.06	67.93
HybridSN [25]	85.03	85.69	83.79	76.71	79.55	75.82
HybridCNN [29]	84.97	85.44	83.47	76.24	78.21	74.42
MS-3DCNN [30]	87.15	87.24	85.74	77.05	80.10	76.72
Proposed Method	88.24	88.13	86.06	78.21	80.93	77.97

TABLE IV. TESTING TIME(SEC) AND TRAINING TIME(MIN) FOR BENCHMARK AND INDIAN DATASETS.

Model	SA		PU		IP		AH-1		AH-2	
	Train	Test	Train	Test	Train	Test	Train	Test	Train	Test
3D-CNN	62	78	52	65	45	52	91	112	92	110
HybridSN	50	64	45	60	40	50	88	104	86	102
HybridCNN	122	27	112	23	74	11	102	120	98	108
MS-3DCNN	80	82	76	68	52	58	93	115	94	113
Proposed Method	75	80	70	65	50	55	90	100	90	102

TABLE V. EFFECT OF THE SPATIAL PATCH DIMENSION ON THE ACHIEVEMENT OF PRESENTED METHOD.

Dataset	Spatial patch sizes		
	$p_1 = 15x15, p_2 = 13x13, p_3 = 11x11$	$p_1 = 13x13, p_2 = 11x11, p_3 = 9x9$	$p_1 = 11x11, p_2 = 9x9, p_3 = 7x7$
SA	99.99	99.21	97.86
PU	99.99	98.93	96.87
IP	99.98	98.82	97.10
AH-1	88.13	86.48	85.76
AH-2	80.93	78.97	77.85

IV. EXPERIMENTAL STUDY AND SNALYSIS

This section provides the datasets descriptions, experimental setups, and experimental evaluation of MS-HybSN model. the details are explained in the following subsections.

A. Description of Datasets

An experimental investigation was carried out using three publicly available HSI datasets: PU (Pavia-University), SA (Salinas), and IP (Indian-Pines). The ground truth is provided with 16 class-labels for the IP dataset, which was recorded from the Indian-Pines test-site in North-western-Indiana During a flying-campaign above Pavia, northern-Italy, PU was captured with 9 class-labels of ground-truth. The ground-truth for the SA was taken with 16 class-labels from the Salinas-Valley. Furthermore, two new Indian datasets, AH1 (Ahmedabad-1) and AH2 (Ahmedabad-2), had been employed to assess the potency of the presented method's performance. These datasets were gathered by the ISRO using AVIRIS-NG sensor [30]. The details are provided in Table 1.

B. Experimental Setup

The experiments are carried out using a GPU with 25-GB RAM on the Google Cloud. The established network MS-HybSN is evaluated by randomly picking 20% of samples as train and 80% as test set from every dataset. In the optimization process, the Adagrad optimizer is employed, as well as a categorical cross-entropy with decay (1e-06) and learning rate (0.001). The approach was trained for 100 epochs using batch size of 32. On each data set, the experiments are recited 10 times and the average outcomes were reported.

C. Classification Results and Analysis

The kappa (K), AA (Average-Accuracy), and OA (Overall-Accuracy) had been incorporated to assess the efficacy of the provided network. Contemporary HSI classification models, like 3D-CNN [7], 2D-CNN [7], HybridSN [24], HybridCNN [28], and MS-3DCNN [29], are compared to the results of the presented MS-HybSN model. The classification accuracy attained by all these approaches is displayed in Table 2. It is identified that the presented model achieved 99.99% OA, 99.99% AA on Salinas, 99.99%

International Journal on Recent and Innovation Trends in Computing and Communication
ISSN: 2321-8169 Volume: 11 Issue: 7s
DOI: https://doi.org/10.17762/ijritcc.v11i7s.7026
***Article Received**: 04 April 2023 **Revised:** 25 May 2023 **Accepted:** 05 June 2023*

OA, 99.98% AA on Pavia, and 99.98% OA, 99.13% AA on IP. In light of assessment measures like K, AA, and OA, Table 2 demonstrates that the presented method's classification efficiency is superior to that of alternative models on the contrast datasets. The outcomes are generated using publicly accessible code for the comparable models, and the accuracies for 2D-CNN, 3D-CNN, HybridSN, HybridCNN, and MS-3DCNN models are taken from their respective articles. The presented model's kappa, AA, and OA values are much superior to those of state-of-the-art models. In almost all circumstances, the presented method outperforms the HybridSN approach. Moreover, HybridSN model used 30% samples and presented method uses 20% samples randomly from each category for the model training.

The studies on two new Indian datasets, AH1 and AH2, are being carried out to ensure that the method is efficient and resilient. We used publicly available code to compare our method against models such as 3D-CNN, HybridSN, HybridCNN, and MS-3DCNN. In order to compare other methods, their code was unavailable. The proposed method achieved 88.13 % OA, 88.24 % AA on AH1 dataset and 80.93 % OA, 78.24 % AA on AH2 dataset. On the new datasets, the provided model improved by 1% to 2%, as shown in Table 3. Table 4 indicates the train and test times for presented model and state-of-the-art approaches. The time spent training is measured in minutes, whereas the time spent testing is measured in seconds. The framework training time is shorter when compared to HybridCNN, but longer when compared to HybridSN and 3DCNN. The model requires substantially more testing time than HybridCNN since it uses more test data. On the AH-1 and AH-2 datasets, the proposed model's test and train durations are significantly more on the new datasets, regardless of the fact that it yields better classification accuracy levels.

Table 5 depicts the cause of spatial patch dimensions on the presented method's efficiency. S. K. Roy [24] conducts similar research and concludes that as the spatial patch size is raised, the model's efficiency diminishes and it becomes computationally infeasible. The model's performance can also be improved by combining features retrieved with a few small-patches utilizing varying spatial sizes. As a result, three patches are used in the proposed work to gradually increase the spatial sizes of the filter for convolution. Since limitations of the computational setup, the investigations in this work are described with three patch sizes as inputs to the presented framework: p_1 x p_1 x d = 15 x 15 x 30 , p_2 x p_2 x d = 13 x 13 x 30 , and p_3 x p_3 x d = 11 x 11 x 30 . The comparison of various accuracies of proposed model with current methods for bench mark datasets and Indian datasets are illustrated in Figure 3. Figure 4, Figure 5, and Figure 6 show the classification maps created by the presented model for benchmark datasets. The classification maps obtained by HybridSN, MS-3DCNN, and the presented approach for the AH-1, and AH-2 datasets are depicted in Figure 7, and Figure 8. It's easier to compare the proposed method's classification maps to those made by other methods. Some parts of the presented model's maps are lesser noisy.

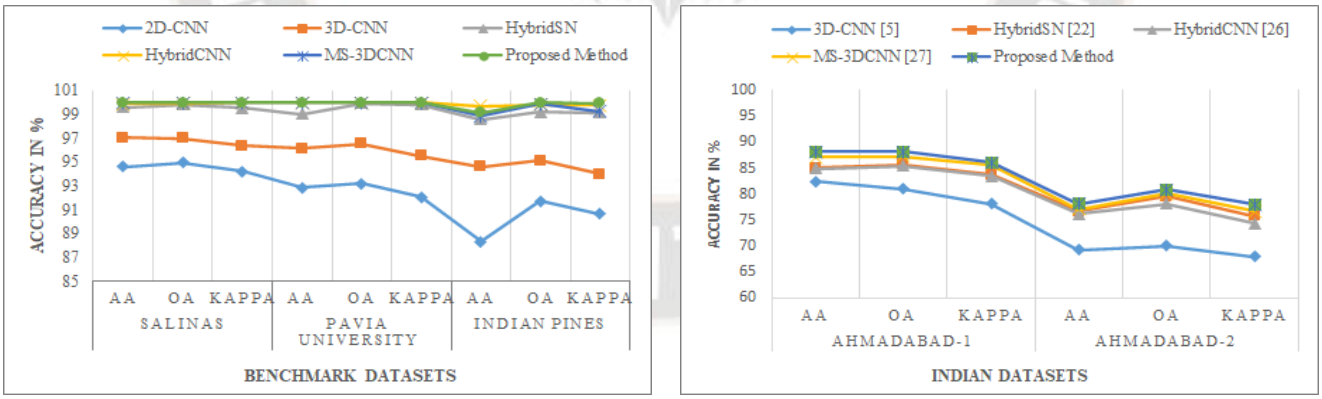

(a) (b)

Figure 3. Comparison of various accuracies of presented model with state-of-art approaches: (a) Benchmark datasets (b) Indian datasets.

International Journal on Recent and Innovation Trends in Computing and Communication
ISSN: 2321-8169 Volume: 11 Issue: 7s
DOI: https://doi.org/10.17762/ijritcc.v11i7s.7026
***Article Received**: 04 April 2023 **Revised:** 25 May 2023 **Accepted:** 05 June 2023*

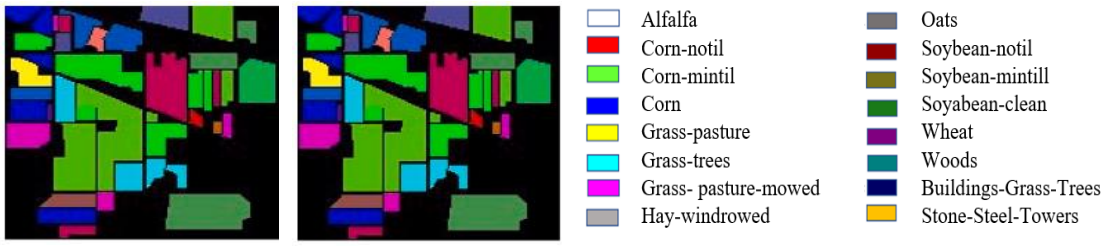

Figure 4. IP (a) image-ground-truth, (b) classification map, (c) indicative class fables.

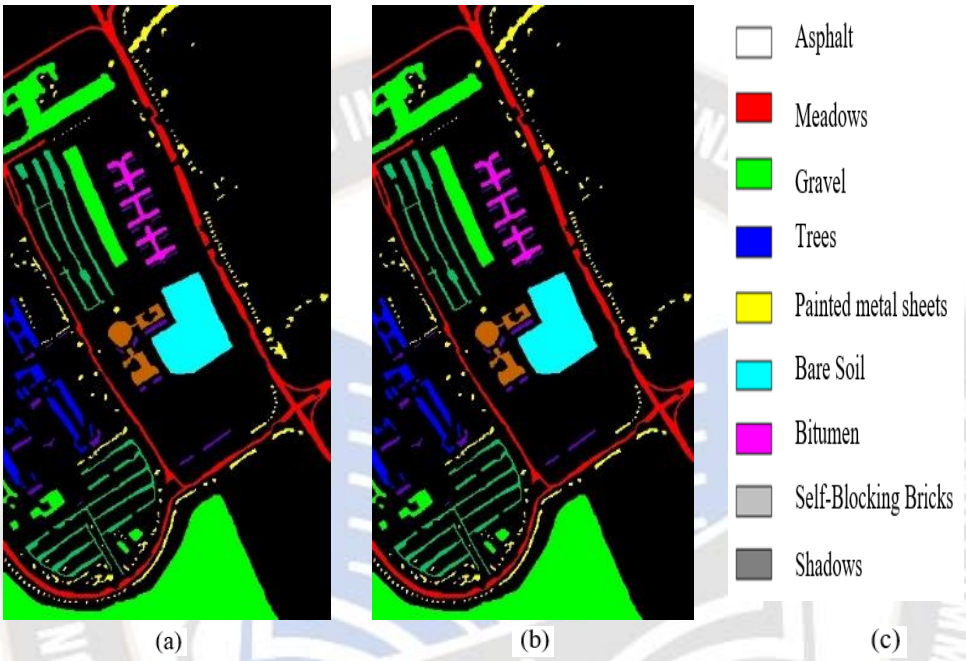

Figure 5. PU (a) image-ground-truth, (b) classification map, (c) indicative class fables.

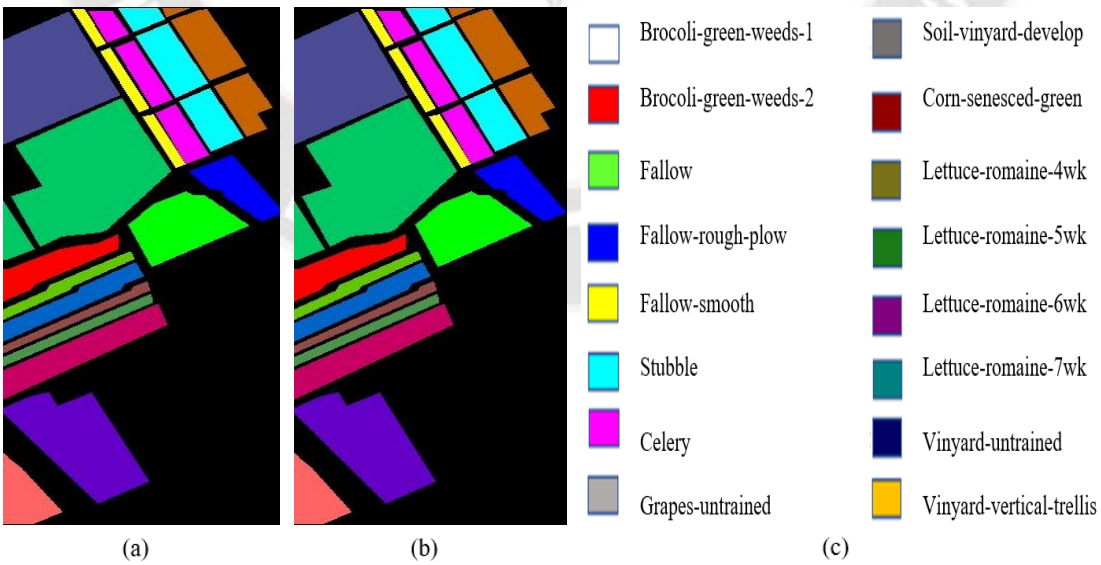

Figure 6. SA (a) image-ground-truth, (b) classification map, (c) indicative class fables.

International Journal on Recent and Innovation Trends in Computing and Communication
ISSN: 2321-8169 Volume: 11 Issue: 7s
DOI: https://doi.org/10.17762/ijritcc.v11i7s.7026
***Article Received**: 04 April 2023 **Revised:** 25 May 2023 **Accepted:** 05 June 2023*

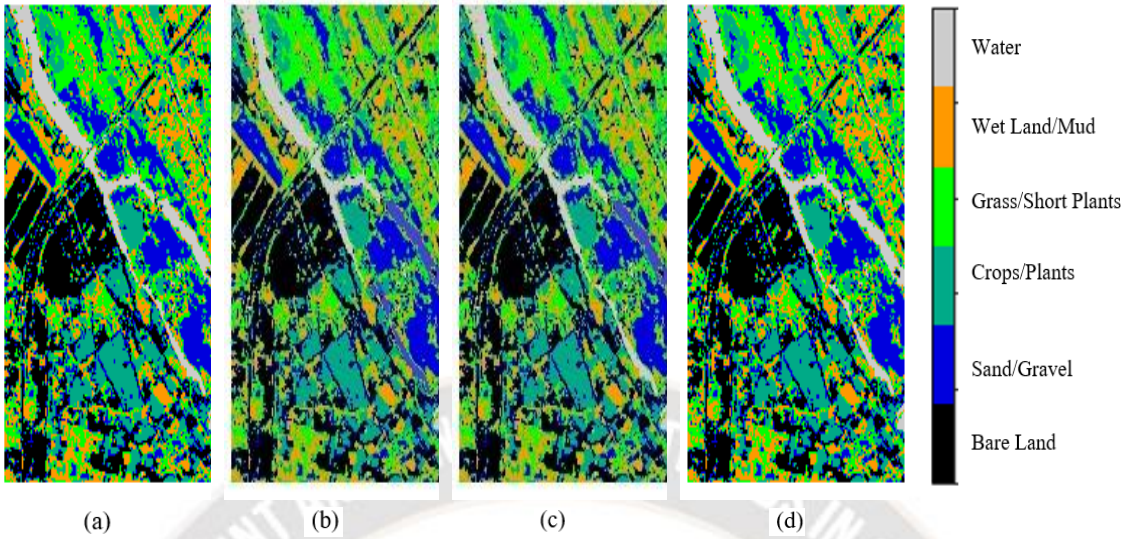

Figure 7. AH-1 (a) image-ground-truth, (b) HybridSN map, (c) MS-3DCNN map, (d) proposed model classification map with indicative class fables.

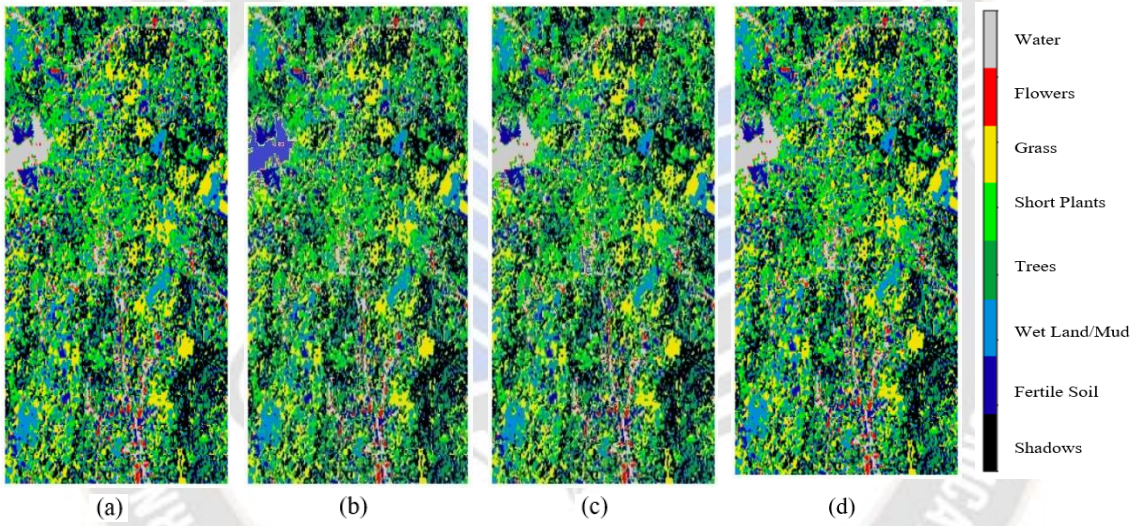

Figure 8. AH-2 (a) image-ground-truth, (b) HybridSN map, (c) MS-3DCNN map, (d) proposed model classification map with indicative class fables.

V. CONCLUSION

Developing a more general deep learning approach for HSI classification is tricky. High classification accuracy may be attained in HSI classification by retrieving deep features from spatial and spectral bands. Although, there is no theoretically sound method for determining the best spatial dimension to examine. Towards this objective, a multiscale hybrid (MS-HybSN) model for HSI classification is recommended in this paper, that extracts deep features in both channels using three separate multi-scale spatial-spectral patches which simply integrates spatial-spectral and spectral data in 3D and 2D convolutions. Experiments on benchmark datasets exhibit that the presented model improves existing models relating to efficiency. The efficiency of the established model is further assessed on new datasets, and it outperforms the HybridSN, HybridCNN, and MS-3DCNN models by a significant margin. The proposed technique exhibited 1%-2% improvement in overall accuracy on benchmark and Indian datasets.

ACKNOWLEDGMENTS

The authors sincerely appreciate help and accept our deepest thanks to Dr. N. Rama Rao, Professor, IIST Trivendrum for supplying AH1 and AH2 datasets.

REFERENCES

[1] M. Imani and H. Ghassemian, "An overview on spectral and spatial information fusion for hyperspectral image classification: Current trends and challenges," Information fusion, Vol. 59, pp. 59–83, 2020, doi: 10.1016/j.inffus.2020.01.007.

[2] S. Prasad and J. Chanussot, "Hyperspectral Image Analysis", Advances in Machine Learning and Signal Processing, Britania Raya, UK: Springer Nature, 2020, doi:10.1007/978-3-030-38617-7.

[3] M. Kanthi, T. H. Sarma, and C. S. Bindu, "A Survey: Deep Learning Classifier for Hyperspectral Image Classification", Journal of Theoretical and Applied Information Technology, Vol. 99, No. 24, pp. 6042-6053, 2021.

[4] Scholkopf, Bernhard, and A. J. Smola, "Learning with kernels: support vector machines, regularization, optimization, and beyond", MIT press, 2018.

[5] Yang, Xiaofei, Y. Ye, X. Li, R. Y. K. Lau, X. Zhang, and X. Huang, "Hyperspectral image classification with deep learning models." IEEE Transactions on Geoscience and Remote Sensing, Vol. 56, No. 9, pp. 5408-5423, 2018, doi: 10.1109/TGRS.2018.2815613.

[6] K. Murali, T. H. Sarma, and C. S. Bindu, "Hybrid learning approach for feature extraction and classification in hyperspectral images", Indian Journal of Computer Science and Engineering (IJCSE), Vol. 12, No. 6, pp. 1559-1567, 2021.

[7] M. E. Paoletti, J. M. Haut, J. Plaza, and A. Plaza, "Deep learning classifiers for hyperspectral imaging: A review", ISPRS Journal of Photogrammetry and Remote Sensing, Vol. 158, pp. 279-317, 2019, doi: 10.1016/j.isprsjprs.2019.09.006.

[8] M. E. Paoletti, J. M. Haut, J. Plaza, and A. Plaza, "A new deep convolutional neural network for fast hyperspectral image classification," ISPRS Journal of Photogrammetry and Remote Sensing, Vol. 145, pp. 120–147, 2018, doi: 10.1016/j.isprsjprs.2017.11.021.

[9] M. Hamouda, K. S. Ettabaa, and M. S. Bouhlel, "Smart feature extraction and classification of hyperspectral images based on convolutional neural networks," IET Image Processing, vol. 14, no. 10, pp. 1999–2005, 2020, doi: 10.1049/iet-ipr.2019.1282.

[10] B. Pan, Z. Shi, and X. Xu, "Mugnet: Deep learning for hyperspectral image classification using limited samples," ISPRS Journal of Photogrammetry and Remote Sensing, Vol. 145, pp. 108–119, 2018, doi: 10.1016/j.isprsjprs.2017.11.003.

[11] L. Fang, N. He, S. Li, A. J. Plaza, and J. Plaza, "A New Spatial–Spectral Feature Extraction Method for Hyperspectral Images Using Local Covariance Matrix Representation," in IEEE Transactions on Geoscience and Remote Sensing, vol. 56, no. 6, pp. 3534-3546, June 2018, doi: 10.1109/TGRS.2018.2801387.

[12] Liu, Bing, X. Yu, P. Zhang, X. Tan, A. Yu, and Z. Xue, "A semi-supervised convolutional neural network for hyperspectral image classification", Remote Sensing Letters, Vol. 8, No. 9, pp. 839-848, 2017, doi:10.1080/2150704X.2017.1331053.

[13] Sarma, Vivek, A. Diba, T. Tuytelaars, and L. V. Gool, "Hyperspectral CNN for image classification & band selection, with application to face recognition", Technical report KUL/ESAT/PSI/1604, KU Leuven, ESAT, Leuven, Belgium, 2016.

[14] Hamida, A. Ben, A. Benoit, P. Lambert, and C. B. Amar, "3-D deep learning approach for remote sensing image classification", IEEE Transactions on geoscience and remote sensing, Vol. 56, No. 8, pp. 4420-4434, 2018, doi: 10.1109/TGRS.2018.2818945.

[15] He, Mingyi, B. Li, and H. Chen, "Multi-scale 3D deep convolutional neural network for hyperspectral image classification", In 2017 IEEE International Conference on Image Processing (ICIP), IEEE, pp. 3904-3908, 2017, doi: 10.1109/ICIP.2017.8297014.

[16] Mrs. Ritika Dhabliya. (2020). Obstacle Detection and Text Recognition for Visually Impaired Person Based on Raspberry Pi. International Journal of New Practices in Management and Engineering, 9(02), 01 - 07. https://doi.org/10.17762/ijnpme.v9i02.83

[17] Liu, Peng, H. Zhang, and K. B. Eom, "Active deep learning for classification of hyperspectral images.", IEEE Journal of Selected Topics in Applied Earth Observations and Remote Sensing, Vol. 10, No. 2, pp. 712-724, 2016, doi: 10.1109/JSTARS.2016.2598859.

[18] Zhu, Jian, L. Fang, and P. Ghamisi, "Deformable convolutional neural networks for hyperspectral image classification.", IEEE Geoscience and Remote Sensing Letters, Vol. 15, No. 8, pp. 1254-1258, 2018, doi: 10.1109/LGRS.2018.2830403.

[19] Yue, Jun, W. Zhao, S. Mao, and H. Liu, "Spectral–spatial classification of hyperspectral images using deep convolutional neural networks.", Remote Sensing Letters, Vol. 6, No. 6, pp. 468-477, 2015, doi: 10.1080/2150704X.2015.1047045.

[20] Zhao, Wenzhi, and S. Du. "Spectral–spatial feature extraction for hyperspectral image classification: A dimension reduction and deep learning approach.", IEEE Transactions on Geoscience and Remote Sensing, Vol. 54, No. 8, pp. 4544-4554, 2016, doi: 10.1109/TGRS.2016.2543748.

[21] Chen, Yushi, H. Jiang, C. Li, X. Jia, and P. Ghamisi, "Deep feature extraction and classification of hyperspectral images based on convolutional neural networks.", IEEE Transactions on Geoscience and Remote Sensing, Vol. 54, No. 10, pp. 6232-6251, 2016, doi: 10.1109/TGRS.2016.2584107.

[22] Lee, Hyungtae, and H. Kwon, "Contextual deep CNN based hyperspectral classification.", In 2016 IEEE international geoscience and remote sensing symposium (IGARSS), IEEE, pp. 3322-3325, 2016, doi: 10.1109/IGARSS.2016.7729859.

[23] Hamida, A. Ben, A. Benoit, P. Lambert, and C. B. Amar, "3-D deep learning approach for remote sensing image classification", IEEE Transactions on geoscience and remote sensing, Vol. 56, No. 8, pp. 4420-4434, 2018, doi: 10.1109/TGRS.2018.2818945.

[24] K. Murali, T. H. Sarma, and C. S. Bindu, "A 3D-deep CNN based feature extraction and hyperspectral image classification.", In 2020 IEEE India Geoscience and Remote Sensing Symposium (InGARSS), IEEE, pp. 229-232, 2020, doi: 10.1109/InGARSS48198.2020.9358920.

[25] Roy, S. Kumar, G. Krishna, S. R. Dubey, and B. Chaudhuri, "HybridSN: Exploring 3-D–2-D CNN feature hierarchy for hyperspectral image classification.", IEEE Geoscience and Remote Sensing Letters, Vol. 17, No. 2, pp. 277-281, 2019, doi: 10.1109/LGRS.2019.2918719.

[26] B. Raviteja, M. S. P. Babu, K. V. Rao, and J. Harikiran, "A New Methodology of Hierarchical Image Fusion in Framework for Hyperspectral Image Segmentation," Indonesian Journal of Electrical Engineering and Computer Science, Vol. 6, No. 1, pp. 58-65, 2017.

[27] S. Wan, C. Gong, P. Zhong, B. Du, L. Zhang, and J. Yang, "Multiscale Dynamic Graph Convolutional Network for

International Journal on Recent and Innovation Trends in Computing and Communication
ISSN: 2321-8169 Volume: 11 Issue: 7s
DOI: https://doi.org/10.17762/ijritcc.v11i7s.7026
***Article Received**: 04 April 2023 **Revised:** 25 May 2023 **Accepted:** 05 June 2023*

Hyperspectral Image Classification.", IEEE Transactions on Geoscience and Remote Sensing, Vol. 58, No. 5, pp. 3162-3177, 2020, doi: 10.1109/TGRS.2019.2949180.

[28] Z. Meng, L. Li, L. Jiao, Z. Feng, X. Tang, and M. Liang, "Fully dense multiscale fusion network for hyperspectral image classification.", Remote Sensing, Vol. 11, No. 22, 2019, doi: 10.3390/rs11222718.

[29] Harris, K., Green, L., Perez, A., Fernández, C., & Pérez, C. Exploring Reinforcement Learning for Optimal Resource Allocation. Kuwait Journal of Machine Learning, 1(4). Retrieved from http://kuwaitjournals.com/index.php/kjml/article/view/155

[30] Viswanathan, D., Kumari, S., & Navaneetham, P. (2023). Soft C-means Multi objective Metaheuristic Dragonfly Optimization for Cluster Head Selection in WSN. International Journal of Intelligent Systems and Applications in Engineering, 11(2s), 88–95. Retrieved from https://ijisae.org/in

[31] Mohan and M. Venkatesan, "HybridCNN based hyperspectral image classification using multiscale spatiospectral features", Infrared Physics & Technology, Vol. 108, 2020, doi: 10.1016/j.infrared.2020.103326.

[32] M. Kanthi, T. H. Sarma, and C. S. Bindu, "Multi-scale 3D-convolutional neural network for hyperspectral image classification.", Indonesian Journal of Electrical Engineering and Computer Science, Vol. 25, No. 1, pp. 307-316, 2022, doi: 10.11591/ijeecs.v25.i1.pp307-316.

[33] M. K. Tripathi and H. Govil, "Evaluation of AVIRIS-NG hyperspectral images for mineral identification and mapping", Heliyon, Vol. 5, No. 11, p. e02931, 2019, doi:10.1016/j.heliyon.2019.e02931.